Research Journal of Pure Science and Technology E-ISSN 2579-0536 P-ISSN 2695-2696
Vol 8. No. 2 2025 www.iiardjournals.org Online version

Diffusion Rate Modelling of Natural Gas Condensate from the Niger Delta Geological Formation in Marine Environment

Hezekiah Andrew Nwosi
Department of Petroleum and Gas Engineering,
Federal University Otuoke, Bayelsa State, Nigeria.
nwosiha@fuotuoke.edu.ng

Wosu Chimene Omeke
Department of Chemical Engineering,
Federal University Otuoke, Bayelsa State, Nigeria.
wosuco@fuotuoke.edu.ng
DOI: 10.56201/rjpst.vol.8.no2.2025.pg19.42

Abstract

A comprehensive mathematical model was developed to monitor and predict the diffusion rate of natural gas condensate within a marine environmental system in the Niger Delta. Specifically utilizing natural gas condensate sourced from the Niger Delta geological formation region of Nigeria. The model is based on a first-order differential equation, which was derived and subsequently solved using the Laplace transformation method. This approach was further refined utilizing partial fraction decomposition, alongside the application of relevant boundary conditions. The model enables the monitoring of concentration of dissolved natural gas condensate components in water over time, as well as determination of the equilibrium concentration of these components. Results from the analysis indicated a notable increase in both the concentration of dissolved hydrocarbon components (C_{HCW}) *and the equilibrium concentration of these hydrocarbons* (C^*_{HCW}) *in the marine environment. Furthermore, the model facilitates predictions of the concentration levels of dissolved hydrocarbons at various residence times* (τ)*. The relationship between the residence time and the concentration of the dissolved hydrocarbon components was meticulously explored, leading to insights into the behavior of these compounds in marine settings. This improved understanding is critical for assessing environmental impacts and developing strategies for effective management of natural gas condensate in aquatic ecosystems. A model was established that yields the slope of the graph effectively. The developed model illustrates the utility of the mathematical equation derived for monitoring, predicting, and evaluating the rate at which natural gas condensate diffuses in marine environments. This approach enhances our understanding of the dispersion dynamics, providing valuable insights for environmental assessments and management strategies related to natural gas spills in aquatic ecosystems.*

***Keywords**: Diffusion, mathematical Model, Natural Gas Condensate, Niger Delta Formation.*

1. Introduction

The marine environment has been utilized in most parts of the world where hydrocarbon mining operations are ongoing and, in most cases, globally as a critical component in the transportation of products and sometimes used for the discharges of contamination in the cause of wastewater treatment. These natural systems leverage the capabilities of microorganisms to effectively break down and eliminate various contaminants. The impact of the petroleum industry on the environment has been a growing concern, particularly regarding the effluents released during different stages of the petroleum lifecycle—including exploration, extraction, transportation, refining, and consumption (Orodu & Orodu, 2011). This activities have significantly contributed to environmental pollution, drawing attention from researchers and policymakers alike. Recent investigations conducted by various research teams highlight a troubling trend: in Nigeria, the surge in petroleum activities has resulted in alarmingly high concentrations of petroleum hydrocarbon contaminants seeping into wastewater from both upstream and downstream operations. This contamination has led to severe disruption within the ecological systems, adversely affecting wildlife and plant life. While some of the pollutants released by the petroleum sector may eventually enter the environment and be subjected to the natural biogeochemical cycles, it is evident that comprehensive measures are imperative for the complete removal of these harmful substances. In an era where environmental quality and food security are of utmost importance, a profound understanding of the behavior and impact of these contaminants is crucial. Comprehensive studies have been conducted on pollutants across various mediums—including wastewater, air, soil, and subsurface systems—revealing that their effects are not only significant but also far-reaching. Addressing these issues is vital for safeguarding our ecosystems and promoting sustainable practices (Adewusi & Ilori 2012).

Investigations have shown that when petroleum or its byproducts are discharged into a marine environment, especially in the Niger Delta, several processes occur that significantly impact the local ecosystem. Initially, the lighter components of natural gas condensate, such as volatile organic compounds, are lost to the atmosphere through evaporation. This not only reduces the number of harmful substances in the water but also contributes to air pollution. Meanwhile, the soluble constituents of the petroleum dissolve into the water column, leading to a deterioration in water quality. As the discharge continues, a thin film of hydrocarbons spreads across the surface of the water, creating an oily sheen that can impede oxygen transfer to aquatic organisms and disrupt photosynthesis in submerged plants (Blunt *et al* 2004). The dissolved components in the water are predominantly medium molecular weight aromatic hydrocarbons, which include compounds such as benzene, toluene, ethylbenzene, and xylene (collectively known as BTEX). These chemicals can be toxic to aquatic life and can bioaccumulate in the food chain. Additionally, these dissolved hydrocarbons tend to migrate and accumulate towards the sediment layer at the bottom of the marine environment over time. This build-up of contaminants poses long-term ecological risks, not only impacting the immediate aquatic environment but also potentially affecting groundwater quality and land-based ecosystems. Mitigating the ecological impact of such discharges is crucial for preserving aquatic habitats and ensuring the health of the surrounding environment (Adaku *et al* 2022).

Numerous microorganisms play a vital role in the degradation of various components of petroleum, a process that has been extensively studied and documented in scientific literature. These microbial systems, consisting of bacteria, fungi, and other microorganisms, offer several beneficial effects through their metabolic activities. Research indicates that these microbes can effectively break down hydrocarbons, resulting in qualitative and quantitative changes in the properties of petroleum across its heavy, medium, and light fractions (Aprioku *et al* 2023). This bioremediation process not only aids in the detoxification of contaminated environments but can also enhance the recovery of valuable resources from petroleum waste. As a byproduct of microbial degradation, various compounds such as oxides of sulfur and nitrogen are produced, alongside traces of metals and non-metallic compounds. These transformations highlight the complex interactions that occur during microbial activity, illustrating their critical role in environmental management and the natural cycling of nutrients. The understanding of these microbial processes paves the way for the development of innovative biotechnological applications aimed at addressing petroleum contamination and promoting ecosystem health (Ifeoluwa *et al* 2019).

The findings from these investigations have garnered significant interest from scientific communities regarding the application of microbes for the enhancement of remediation processes aimed at addressing contaminants found in both marine and terrestrial environments. Research into bioremediation, particularly in Nigerian ecosystems, has concentrated on its design methodologies, modeling techniques, and simulations focused on the biodegradation of crude oil. It is challenging to produce a definitive and comprehensive analysis of the bioremediation of petroleum hydrocarbon-contaminated environments unless a well-defined design model and an appropriate remediation approach are established. Comprehensive studies have been conducted on hydrocarbons present in the terrigenous and calcareous sediments of the two lagoons: Grand Cul-de-Sac Marine and Petit Cul-de-Sac Marine. Sampling and analysis of these sediments revealed alarmingly high concentrations of organic matter and hydrocarbons. The investigative results indicated that the surface sediments of these lagoons predominantly consist of n-alkanes. Specifically, the sediments from Petit Cul-de-Sac Marine (PCSM) are notably affected by pollution from petroleum hydrocarbons. In contrast, Grand Cul-de-Sac Marine (GCSM) exhibits a linear fraction that is chiefly characterized by n-alkanes originating from higher plants or seagrasses. Furthermore, the polycyclic aromatic hydrocarbons (PAHs) identified in these sediments are primarily indicative of residues from combustion processes. The distribution patterns and sources of non-aromatic hydrocarbons (NAHs) and polycyclic aromatic hydrocarbons (PAHs) have been meticulously examined by various research teams, shedding light on the complex interactions between pollutants and sediment composition in these ecologically significant marine environments (Aust *et al*, 2004).

The environmental impact of oil exploration and exploitation represents a significant consequence of economic development in our modern, technologically driven age. In Nigeria, for instance, the extraction of crude oil has led to widespread contamination of both aquatic and terrestrial ecosystems. This contamination not only disrupts local wildlife but also adversely affects the livelihoods of communities that depend on these ecosystems for sustenance and economic activities. The mechanisms of oil dispersion are complex; wind and wave action play crucial roles in transporting oil from offshore extraction sites to vulnerable shorelines, exacerbating the environmental damage. The consequences of oil spills and leaks extend beyond immediate visual pollution; they can lead to long-term degradation of habitats, loss of biodiversity, and alterations in the ecological balance within these regions. Research conducted by various environmental and scientific organizations has meticulously analyzed the discharge of petroleum and petroleum products into the surrounding environment caused by the full cycle of oil production (Botwe & Akpabio, 2020). This cycle encompasses exploration, extraction, transportation, refining, and the eventual utilization of oil. Each stage presents specific risks to the environment, highlighting the urgent need for sustainable practices and policies to mitigate these impacts and protect affected ecosystems for future generations (Afolabi *et, al* 2020)

2. Materials and Methods

The rate at which hydrocarbons disperse, or diffuse, can be articulated through three key components: longitudinal mass flux, which refers to the movement of mass along the direction of flow; vertical mass flux, indicating the transfer of mass in an upward or downward direction; and transverse mass flux, which describes the flow of mass across the primary direction of movement. Each of these flux components plays a crucial role in understanding the overall dispersion dynamics of hydrocarbons in various environments.

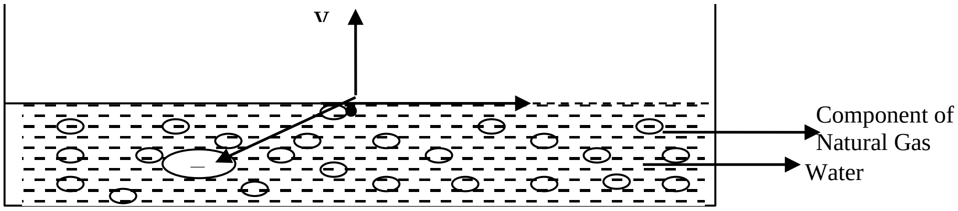

Figure 1. A sample of marine environment and natural gas condensate diffusing in x, y and z-directions

An enhanced model, building upon the foundational framework of diffusion and dispersion rates of petroleum hydrocarbons, is illustrated in the following sections. This updated approach delves deeper into the intricacies of how these substances spread through various environments, providing a more comprehensive understanding of their dynamics and interactions within ecological systems.

$$\text{Longitudinal mass flux} = \left(\phi_x C - E_x \frac{\partial c}{\partial x}\right) \tag{1}$$

$$\text{Vertical mass flux} = \left(\phi_y C - E_y \frac{\partial c}{\partial y}\right) \tag{2}$$

$$\text{Transverse mass flux} = \left(\phi_z C - E_z \frac{\partial c}{\partial z}\right) \tag{3}$$

E_x, E_y, E_z = represent the turbulent or eddy diffusion coefficients in the x, y, and z directions, respectively. These coefficients quantify the rate at which momentum, energy, or mass is transported due to eddies in the fluid flow. $\phi_{x,}$ $\phi_{y,}$ $\phi_{z,}$ = bulk velocities, the bulk velocities in each direction are denoted as $\phi_{x,}$ $\phi_{y,}$ $\phi_{z,}$ indicating the average velocities of the fluid flow in the x, y, and z directions. C = stands for the concentration of dispersed natural gas condensate within the medium. To analyze the movement and impact of these hydrocarbons, we can sum the fluxes of the substances across the domain. By applying the principle of material balance and accounting for the change in concentration over time, we can formulate a comprehensive equation. This equation allows us to understand how the concentration of petroleum hydrocarbons evolves, influenced by both diffusion processes and bulk flow dynamics. This approach is essential for accurately modeling the dispersion and potential environmental impact of petroleum hydrocarbons in various settings.

$$\frac{\partial c}{\partial t} = -\frac{\partial}{\partial x}\left(\phi_x C - E_x \frac{\partial c}{\partial x}\right) - \frac{\partial}{\partial y}\left(\phi_y C - E_y \frac{\partial c}{\partial y}\right) - \frac{\partial}{\partial z}\left(\phi_z C - E_z \frac{\partial c}{\partial z}\right) + S_1 \qquad (4)$$

The variable S1 represents a function of the three dimensions: x, y, and z, mathematically expressed as S1 = f (x, y, z). This notation is utilized to signify the external forces acting on a system, particularly concerning the rate of transfer of various elements, such as wind currents or other environmental factors. By expanding equation (4), we can gain deeper insights into how these external forces influence the dynamics of the system under study, providing a more comprehensive understanding of the interactions at play.

$$\frac{\partial c}{\partial t} = -\,\phi_x \frac{\partial}{\partial x} + \frac{E_x \partial^2 C}{\partial x^2} - \phi_y \frac{\partial c}{\partial y} + E_y \frac{E_x \partial^2 C}{\partial y^2} - \phi_z \frac{\partial}{\partial z} + E_z \frac{E_x \partial^2 C}{\partial z^2} + S_1 \qquad (5)$$

In our analysis of a marine environment characterized by the diffusion of petroleum hydrocarbons, we focus on the specific conditions where bulk diffusion is absent. Under these circumstances, the bulk velocity of the fluid is effectively zero, which significantly influences the diffusion process. Consequently, this leads us to refine our understanding of the relevant equations governing this phenomenon. As a result, equation (5) can be simplified to reflect these conditions, allowing us to better capture the dynamics of hydrocarbon diffusion in this stagnant environment (Ojo & Tse, 2023).

$$\frac{\partial c}{\partial t} = E_x \frac{\partial^2 C}{\partial x^2} + E_y \frac{\partial^2 C}{\partial y^2} + E_z \frac{\partial^2 C}{\partial z^2} + S_1 \qquad (6)$$

To analyze the rate of hydrocarbon dispersion or diffusion as described in equation (6), we will focus specifically on a two-dimensional model, taking into account the X and Y directions. This approach allows us to simplify the complexity of the diffusion process by reducing it to a plane, thereby enhancing our understanding of how hydrocarbon molecules spread through a given area. By applying the principles of diffusion theory in both the X and Y dimensions, we can derive a more comprehensive representation of the dispersion dynamics at play.

$$\frac{\partial c}{\partial t} = E_x \frac{\partial^2 C}{\partial x^2} + E_y \frac{\partial^2 C}{\partial y^2} \tag{7}$$

In analyzing the rate of dispersion or diffusion, we will focus exclusively on the X and Y directions, as illustrated in Figure 3.6. This two-dimensional perspective allows us to understand how substances spread across a plane over time. By examining the concentration gradients and the factors influencing diffusion in these specific directions, we can gain insights into the underlying mechanisms that govern the movement of particles. This approach will help us better comprehend the dynamics at play within the system being studied.

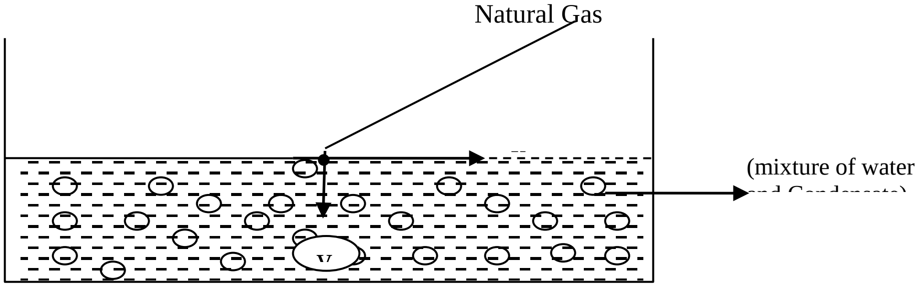

Figure 2 illustrates a sample of a marine environment where natural gas condensate hydrocarbon mixtures are diffusing primarily in the x and y directions. To define E about K3, we have the equation K_3; ($E = K_3$). The expression for E as a function of x and y is given by:

E (x, y) = K (3x, 3y) A1

$$E_{(x,\,y)} = K_{(3x,\,3y)} A_1 \tag{8}$$

During the initial spreading phase of the hydrocarbons, before the system reaches equilibrium, the rate of diffusion in the x-direction (K3x) is significantly greater than the rate in the y-direction (K3y). This indicates that the horizontal transfer of the hydrocarbon slick is predominant during the spreading stage, where hydrocarbons are rapidly moving outwards from the source. As a result, we can simplify our understanding of the hydrocarbon dispersion model by reducing the analysis to the x-direction alone. Consequently, the previously established Equation (7) can be modified to reflect this one-dimensional flow, focusing solely on the horizontal transfer.

$$\frac{\partial c}{\partial t} = K_{3x} A_1 \frac{\partial^2 C}{\partial x^2} + S_1 \tag{9}$$

Where $E_x = K_{3x} A_1$

At the conclusion of the spreading stage, when a state of equilibrium has been established—indicated by the condition K3xy being significantly greater than K3x—the equation (9) simplifies to a more manageable form. This scenario highlights the dominance of K3xy in the system, allowing us to draw clearer insights from the reduced equation.

$$\frac{\partial c}{\partial t} = K_{3y} A_1 \frac{\partial^2 C}{\partial y^2} \Rightarrow \quad Fick's\ law \tag{10}$$

Fick’s law describes the principles governing the diffusion process, specifically outlining how the mass transfer rate of a hydrocarbon slick dispersing in water can be quantified. This law states that the rate of mass transfer is proportional to the concentration gradient of the substance involved. In the context of hydrocarbons diffusing in water, this means that the flow of hydrocarbons from a region of higher concentration to one of lower concentration occurs at a rate that is directly related to the difference in concentration between the two areas. This relationship can be mathematically expressed to assess the efficiency and dynamics of the diffusion process in aquatic environments, which is crucial for understanding the environmental impact of hydrocarbon spills.

$$N_{HC} = -K_{3y}A_1(C_{HC} - C^*_{HCW}) \tag{11}$$

The equation (11) can be solved by taking into account specific boundary conditions that are essential for ensuring accurate and meaningful results. These boundary conditions define the limits and constraints of the problem, allowing us to apply appropriate mathematical techniques to obtain a solution. An illustration of these conditions is provided below, clearly demonstrating how they interact with the equation and contribute to the overall analysis. By carefully considering these aspects, we can gain a deeper understanding of the behavior of the system described by the equation.

$$\text{at, } t = 0; \quad C_{HCW} = C_{HC} \text{ for all } y \tag{12}$$
$$\text{at, } t \geq 0; \quad C_{HCW} = C^*_{HC} \text{ at } y = 0 \tag{13}$$
$$\text{at, } t \geq 0; \quad C_{HCW} = C_{HC} \text{ at } y = \infty \tag{14}$$

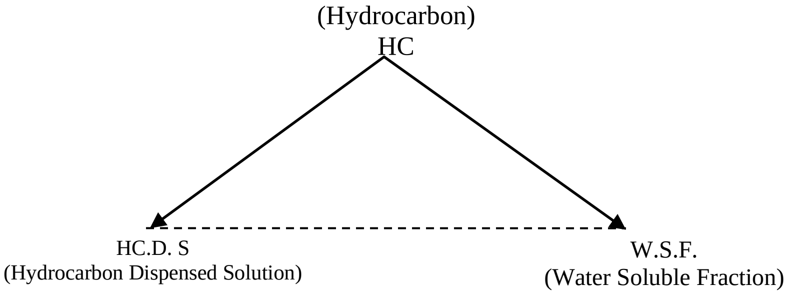

Figure 3: The Triangle Representation of Hydrocarbon Dispersion and Water-Soluble Fraction

This figure illustrates the dynamic relationship between hydrocarbon dispersion and the water-soluble fraction in aquatic environments. The triangle serves as a visual framework to showcase how various concentrations of hydrocarbons can influence their dispersion in water, as well as the proportion of those hydrocarbons that are soluble in water. On one vertex, we have hydrocarbon dispersion, indicating the spread of oil droplets throughout the water column. The second vertex denotes the water-soluble fraction, highlighting the components of hydrocarbons that dissolve in water, potentially affecting aquatic organisms and ecosystems. The third vertex represents the interaction between these two phases, emphasizing the balance between hydrocarbon presence and its bioavailability in marine environments. This triangular model aids in understanding the environmental impact of hydrocarbon spills and guides remediation strategies.

$$\left\{\begin{matrix}\text{The rate of change of}\\ \text{moles of hydrocarbon}\\ \text{per unit time}\end{matrix}\right\} = \left\{\begin{matrix}\text{Moles of volatile}\\ \text{component}\end{matrix}\right\} + \left\{\begin{matrix}\text{Number of moles of}\\ \text{diffused component in}\\ H_2O.\end{matrix}\right\}$$

$$\frac{dN_{HC}}{dt} = -A_{HCa}K_4(C_{HC} - C_{HCa}) - A_{HCW}K_5(C_{HC} - C_{HCW}) \qquad (15)$$

i.e.

$$V_{HCW}\frac{dC_{HCW}}{dt} = -A_{HCa}K_4(C_{HC} - C_{HCa}) - A_{HCW}K_5(C_{HC} - C_{HCW}) \quad \text{Since} \qquad (16)$$

$$\text{Concentration} = \frac{\text{Number of moles}}{\text{volume in } 1dm^3} \qquad (17)$$

According to equation (17), the moles of volatile components within petroleum hydrocarbon fractions do not permeate into the water; rather, they transition into the atmosphere through vaporization. This phenomenon occurs because these volatile components tend to escape into the air rather than dissolve in the aqueous phase. Consequently, the rate at which these petroleum hydrocarbon fractions are transferred to the water is minimal, rendering their influence on water contamination negligible. As a result, equation (17) can be simplified to reflect this reduced transfer rate, highlighting the predominance of vaporization over diffusion in the behavior of these volatile substances.

$$V_{HCW}\frac{dC_{HCW}}{dt} = -K_5A_{HCW}(C_{HC} - C_{HCW}) \qquad (18)$$

To solve Equation (18), one can begin by gathering all similar terms. This process involves arranging the equation systematically and consolidating terms that share the same variable or constant values, which simplifies the equation and facilitates finding the solution.

$$\left(\frac{dC_{HCW}}{C_{HC} - C_{HCW}}\right) = -K_5\left(\frac{A_{HCW}}{V_{HCW}}\right)dt \qquad (19)$$

$$If\ \tau = \left(\frac{-V_{HCW}}{A_{HCW} K_5} \right) \tag{20}$$

By substituting the expression from equation (19) into equation (20), we can derive deeper insights into the relationship between the variables involved. This process allows us to analyze how the changes in one equation affect the other, ultimately leading to a more comprehensive understanding of the underlying mathematical framework. Specifically, we will see how the parameters interact, which can reveal important implications for our overall analysis.

$$\tau \frac{dC_{HCW}}{dT} + C_{HCW} = C_{HC} \tag{21}$$

Equation (21) is classified as a first-order differential equation, characterized by its dependence on initial conditions and a single derivative term. In this equation, the variables (iota) and (C_{HC}) represent constants that affect the behavior of the solution. To solve this equation effectively, we will employ the Laplace transformation technique. This approach allows us to convert the differential equation into an algebraic equation in the Laplace domain, making it simpler to manipulate and solve. Once we obtain the solution in this domain, we can apply the inverse Laplace transformation to revert to the original time domain, providing a complete representation of the system's dynamics.

Where,

$$\frac{dC_{HCW}}{dT} = SC_{HCW(S)} - C_{HCW}(0) \tag{22}$$

$$C_{HCW} = C_{HCW(S)} \tag{23}$$

$$C_{HC} = {C_{HC}}/{S} \tag{23a}$$

By substituting equations (22), (23), and (23a) into equation (21), we can derive a more comprehensive understanding of the interactions among the variables involved. This process involves a careful examination of how each equation contributes to the overall framework presented in equation (21). By integrating these equations, we can clarify the relationships between the different parameters, allowing us to identify any potential implications or outcomes that may arise from these substitutions. This analytical approach not only enhances our grasp of the underlying concepts but also sets the stage for further exploration and analysis of the system at hand.

$$\tau(SC_{HCW(S)} - C_{HCW}(0)) + C_{HCW(S)} = {C_{HC}}/{S} \tag{24}$$

To begin our analysis, let’s take into account the initial condition outlined in our study, which specifies that ($C_{HCW}(0) = 0$). By substituting this initial condition into equation (24), we can derive important insights about the behavior of the function at this starting point. This step is crucial, as it allows us to establish a baseline for further calculations and understand the implications of (C_{HCW}) at time zero. The result of this substitution will also facilitate our exploration of how the system evolves and how (C_{HCW}) responds to varying inputs or conditions in subsequent iterations.

$$\tau(SC_{HCW(S)} - 0) + C_{HCW(S)} = {}^{C_{HC}}\!/_{S} \qquad (25)$$

$$\tau SC_{HCW(S)} + C_{HCW(S)} = {}^{C_{HC}}\!/_{S} \qquad (26)$$

$$(\tau S + 1)C_{HCW(S)} = {}^{C_{HC}}\!/_{S} \qquad (26a)$$

To derive the formula with CHCW(S) as the subject, we start from equation (26a). This involves isolating CHCW(S) on one side of the equation, which may require various algebraic manipulations such as adding, subtracting, multiplying, or dividing both sides by specific terms. By carefully rearranging the equation and ensuring that all operations maintain equality, we will ultimately express CHCW(S) explicitly in terms of the other variables present in the equation. This process not only clarifies the relationship of CHCW(S) to the other components.

$$C_{HCW(S)} = \frac{C_{HC}}{S(\tau S + 1)} \qquad (26b)$$

To solve equation (26b), we will utilize the technique of partial fraction decomposition. This method involves expressing the complex rational expression as a sum of simpler fractions, which can then be more easily analyzed and integrated. First, we will factor the denominator of the expression, identifying the distinct linear and/or irreducible quadratic factors. Once the factors are determined, we will set up the partial fraction decomposition by assigning variables to each fraction corresponding to the factors. After that, we can solve for these variables through either a system of equations or by equating coefficients. This step-by-step approach will allow us to break down the original equation into more manageable parts, ultimately leading to a clearer solution and deeper understanding of the underlying problem.

$$\frac{C_{HC}}{S(\tau S + 1)} = \frac{A}{S} + \frac{B}{\tau S + 1} \qquad (26c)$$

Let (A) and (B) represent constants in our analysis. By examining equation (26c) more closely, we can extract several important insights. This equation highlights the relationship between the variables involved, and understanding its structure can help us predict the behavior of the system under various conditions. Additionally, the constants (A) and (B) play a crucial role in determining the dynamics of the equation, influencing both stability and responsiveness in different scenarios. To fully grasp the implications of equation (26c), we must consider how changes in these constants can affect the overall behavior of the system being modeled.

$C_{HC} = A\ (\iota S + 1) + BS$ (27)

To begin our analysis, we start by setting the value of (S) to zero. Substituting this value into equation (27) allows us to explore the implications and outcomes that arise from this initial condition. This equation is pivotal to our discussion, as it will provide us with the foundation to draw further conclusions and insights. By placing (S = 0) into the equation, we can systematically evaluate the resulting expression and its impact on the overall analysis.

$C_{HC} = A\ (\iota \times 0 + 1) + B\ (0)$

$C_{HC} = A\ (0 + 1) + B\ (0)$

$C_{HC} = A + 0 \quad \therefore\ A = C_{HC}$ (28)

Also, Let S = - $\frac{1}{\tau}$, Incorporating this specific value into equation (27) allows us to analyze its impact on the overall calculations. By substituting the numerical value, we can better understand how it influences the equation's outcomes and subsequently interpret the results in the context of our study.

$$C_{HC} = A\left(\tau x - \frac{1}{\tau} + 1\right) + B\left(-\frac{1}{\tau}\right) \tag{29}$$

$$C_{HC} = A(-1+1) + B\left(-\frac{1}{\tau}\right)$$

$$C_{HC} = A(0) + B\left(-\frac{1}{\tau}\right)$$

$$C_{HC} = 0 - \frac{B}{\tau} \quad \therefore \text{ B = - ι}C_{\text{HC}} \tag{30}$$

By substituting the values obtained from equations (28) and (30) into equation (26c), we can derive a more comprehensive understanding of the relationships among these variables. This substitution allows us to simplify equation (26c) and explore how the parameters influence the overall system. Specifically, we will analyze the resulting expression to identify any new insights or implications that arise from this integration of equations.

$$\frac{C_{HC}}{S(\tau S+1)} = \frac{C_{HC}}{S} - \frac{\tau C_{HC}}{(\tau S+1)} \tag{31}$$

To clarify and simplify equation (31), we begin by breaking down its components step by step. This process will help reveal the underlying relationships and make it easier to understand the equation’s structure and implications. Let's explore each part of the equation in detail to achieve a clearer and more concise representation.

$$C_{HCW(S)} = \frac{C_{HC}}{S} - \frac{\tau C_{HC}}{(\tau S+1)} \tag{32}$$

$$C_{HCW(S)} = \frac{C_{HC}}{S} - \frac{\tau C_{HC}}{\tau\left(S + \frac{1}{\tau}\right)} \tag{33}$$

$$C_{HCW(S)} = \frac{C_{HC}}{S} - \frac{\tau C_{HC}}{\left(S + \frac{1}{\tau}\right)} \tag{34}$$

To express equation (34) in the time domain, we need to perform an inverse Laplace transform on the given equation. This process involves determining the original time-dependent function that corresponds to the transformed equation when defined in the Laplace domain. By carefully applying the appropriate inverse Laplace techniques and, if necessary, utilizing known transforms or tables, we can derive a clearer and more comprehensive representation of the system's behavior over time. This transformation will enable us to analyze the dynamic response and other relevant characteristics in the time domain more effectively.

$$C_{HCW(t)} = C_{HC} - C_{HC}\,\ell^{-\left(\frac{t}{\tau}\right)} \tag{35}$$

$$C_{HCW(t)} = C_{HC}\left(1 - \ell\right)^{-\left(\frac{t}{\tau}\right)} \tag{36}$$

By dividing equation (36) by the variable CHC, we can simplify the expressions involved and gain clearer insights into the relationships between the variables. This operation allows us to isolate terms and analyze their contributions more effectively. Let's explore the implications of this division on the overall equation and how it can help us better understand the underlying dynamics.

$$\frac{C_{HCW(t)}}{C_{HC}} = \frac{C_{HC}}{C_{HC}} \; \frac{C_{HC}}{C_{HC}}\,\ell^{-\left(\frac{t}{\tau}\right)} \tag{37}$$

$$\frac{C_{HCW(t)}}{C_{HC}} = 1 - \ell^{-\left(\frac{t}{\tau}\right)} \tag{38}$$

$$\left(\frac{C_{HCW(t)}}{C_{HC}} - 1\right) = \ell^{-\left(\frac{t}{\tau}\right)} \tag{39}$$

Or

$$\left(1 - \frac{C_{HCW(t)}}{C_{HC}}\right) = \ell^{-\left(\frac{t}{\tau}\right)} \tag{40}$$

By applying the logarithmic function to both sides of equation (40), we can transform the equation into a more manageable form. This step is particularly useful because it allows us to leverage the properties of logarithms, such as converting products into sums and powers into products. Consequently, we can simplify our analysis and solve for the desired variable more effectively. The resulting expression will provide us with valuable insights into the underlying relationships within the equation.

$$In\left(1 - \frac{C_{HCW(t)}}{C_{HC}}\right) = -\frac{t}{\tau} \tag{41}$$

2.1 Sample Collection

A sample of the fresh effluent was meticulously collected and transferred into sterilized sample bottles to prevent any contamination. This was done to ensure an accurate analysis of the individual hydrocarbon components and other relevant parameters outlined previously. The collection process involved using appropriate protective equipment and following standardized protocols to maintain the integrity of the sample. Upon transfer, the bottles were sealed securely and labeled with pertinent information, including the date, time, and location of collection, to facilitate traceability and reference during laboratory analysis. This comprehensive approach aims to provide a detailed understanding of the effluent's chemical composition and potential environmental impact (Oburoh *et al*, 2017):

2.1.1 pH Test

The significance of the pH level of effluent discharged into a marine environment plays a crucial role in the ecological balance and health of the aquatic environment. Specifically, extreme pH values—whether high or low—can significantly impact the growth rates of microorganisms that are essential for maintaining the marine environment's ecosystem. Most microorganisms thrive within a specific pH range, typically around neutral (pH 6.5 to 7.5). When the pH strays too far from this range, it can be detrimental to their survival and reproduction. For instance, many species of bacteria and algae cannot withstand high pH levels (above 9.0), which can lead to a decline in their populations. Conversely, excessively low pH levels (below 6.0) can also prove fatal for various microorganisms, limiting their ability to contribute to nutrient cycling and organic matter breakdown. Consequently, maintaining an optimal pH level is vital for promoting healthy microbial communities, which in turn supports the overall health of the pond ecosystem. Efforts to monitor and manage pH levels in effluent are essential for sustaining the delicate balance of aquatic life and ensuring the long-term viability of the marine environment.

pH Measurement: Procedure and Equipment

Importance of pH: pH is a critical factor in various chemical processes, environmental studies, and treatment methods, as it significantly influences the behavior of solutes in solution, microbial activity, and the efficacy of chemical reactions. Essential Equipment: pH Meter: An instrument that measures the hydrogen ion concentration in a solution, providing an accurate pH reading. Magnetic Stirrer: A device that uses a rotating magnetic field to stir solutions, ensuring homogeneity during measurement. Materials Required: Buffer Solutions: Standardized solutions with known pH values, specifically pH 7 (neutral) and pH 4 (acidic), are used for calibration. Effluent Samples: The samples whose pH levels need to be determined are typically collected from environmental sources or industrial discharge.

Procedure for measuring pH: 1. Standardization of the pH Meter: Before starting the measurement process, it is essential to calibrate the pH meter to ensure accurate readings. This involves rinsing the electrode with distilled water and then immersing it in a buffer solution of pH 7. Adjust the pH meter according to the manufacturer’s instructions to align the reading with the known pH of the buffer. After the calibration with pH 7 is complete, rinse the electrode again and proceed to check its accuracy using the pH 4 buffer solution to confirm that the meter is functioning properly across the required range. 2. Preparation of Effluent Samples: Pour a sample of the buffer solution with a pH of 7 into a clean beaker to prepare for measurement. Measure and record the temperature of both buffer solutions (pH 4 and pH 7) as temperature can affect pH readings. 3. Measuring the pH of Effluent Samples: With the pH meter properly calibrated, place the electrode into the effluent sample contained within a clean beaker. Use the magnetic stirrer to gently mix the sample for approximately one minute, ensuring that the solution is well-mixed and the electrode is adequately exposed to the solution. Allow the pH meter to stabilize and then record the pH value displayed. We repeated this step for each effluent sample, ensuring thorough cleaning of the electrode between measurements to prevent cross-contamination. 4. Final Steps: After completing the measurements, clean the pH electrode according to the manufacturer's guidelines and store it properly to maintain its longevity and performance. By following this detailed procedure, accurate and reliable pH readings can be achieved, facilitating further analysis and decision-making based on the chemical characteristics of the effluent samples.

2.1.2 Hydrocarbon Analysis

Significance**:** Understanding the precise composition of individual hydrocarbons present in a sample is crucial, as it directly influences the assessment of the sample's toxicity levels. By identifying the specific components within the effluent, we can strategically design an effective bioremediation program tailored to mitigate the environmental impact of these hydrocarbons. This detailed analysis not only informs the decision-making process for remediation strategies but also aids in predicting the potential ecological risks associated with various hydrocarbon types. Furthermore, conducting a thorough examination of the concentration of petroleum hydrocarbons allows researchers and environmental scientists to gauge the extent of contamination, guiding remediation efforts and evaluating the efficacy of the proposed solutions. This aspect is crucial as it allows us to effectively assess the progress of the bioremediation program and make informed decisions based on the data collected. Major Equipment: 1. Infrared Detector: Utilized to identify and quantify specific gaseous compounds, enabling us to monitor the presence of hydrocarbons in the environment. 2. Thermometer: Essential for measuring temperature variations, which can affect the bioremediation processes and the behavior of the hydrocarbons. 3. Gas Chromatography (GC): A key analytical technique for separating and analyzing compounds in a gas mixture, providing detailed information on the concentration and types of hydrocarbons present in the samples. Materials: Sample Collection: Precise collection of hydrocarbon mixtures is conducted to ensure representative samples are obtained for analysis. Gas Mixture Cylinder: This cylinder is used to store and transport the collected samples, maintaining their integrity until analysis. Procedure: Hydrocarbon mixtures are subjected to detailed analysis using gas chromatography. During this process, samples are injected into the GC system, where they are vaporized and carried through a column by an inert gas. As the various components in the hydrocarbon mixture interact differently with the column material, they are separated and arrive at the detector at different times. This allows for the identification and quantification of individual hydrocarbons, helping us establish their concentration levels and chemical composition. The findings from this analysis are critical for evaluating the effectiveness of the bioremediation efforts.

2.1.3 The Rate of Diffusion of Petroleum Hydrocarbon Analysis

Significance: The study examines the overall mass transfer of petroleum hydrocarbons across the hydrocarbon-water interface over time, which is a crucial aspect in understanding the behavior and movement of these contaminants in aquatic environments. The findings will provide valuable insights into determining the most effective point of inoculation for remediation efforts, informed by the concentration gradients observed in the samples. Procedure: To conduct this analysis, samples were systematically collected from designated locations within the contaminated area. Each site was selected based on varying levels of hydrocarbon concentration to ensure a comprehensive examination of diffusion rates. Following collection, the samples were subjected to rigorous analytical techniques, as previously outlined, to quantify the concentration of petroleum hydrocarbons in both hydrocarbon and water phases. This methodical approach allows for a thorough understanding of how natural gas condensates disperse with their surrounding environment.

Table 1: Individual Hydrocarbon concentration analysis results

Component	Sample A $(C_{HC})_A$ mol%	Sample B $(C_{HC})_B$ mol%	Sample C $(C_{HC})_C$ mol%	Sample D $(C_{HC})_D$ mol%
1-c4	0.00	0.00	0.00	0.00
n-c4	0.00	0.00	0.00	0.00
i-c5	0.00	0.00	0.00	0.00
n-c5	0.00	0.00	0.00	0.00
C6	0.051	0.013	0.022	0.018
C7	0.26	0.190	0.14	0.11
C8	2.00	1.65	1.40	1.31
C9	6.13	5.27	4.68	4.59
C10	11.62	11.02	10.50	9.99
C11	11.98	11.07	10.68	10.32
$C12^{+}$	67.96	70.77	72.58	73.68

Table 2: Concentration of dissolved hydrocarbon $C_{HCW} = C_{HC} - C_{HC}\ell^{-\frac{t}{\tau}}$ at constant coefficient

		Concentration of dissolved hydrocarbon $C_{HCW} = C_{HC} - C_{HC}\ell^{-\frac{t}{\tau}}$				
Time (hr)	HC component	A	B	C	D	Coefficient of the τ (hr^{-1})
0.30	C6	0.013	0.009	0.006	0.005	0.9
1.00		0.034	0.020	0.014	0.012	0.9
1.30		0.039	0.023	0.017	0.014	0.9
2.00		0.045	0.027	0.020	0.016	0.9

2.30		0.047	0.028	0.020	0.017	0.9
0.30		0.074	0.054	0.040	0.031	0.9
1.00		0.174	0.127	0.094	0.074	0.9
1.30	C7	0.199	0.145	0.107	0.084	0.9
2.00		0.232	0.169	0.125	0.099	0.9
2.30		0.240	0.175	0.129	0.101	0.9
0.30		0.568	0.469	0.398	0.372	0.9
1.00		1.342	1.107	0.939	0.879	0.9
1.30	C8	1.528	1.261	1.070	1.007	0.9
2.00		1.784	1.472	1.249	1.169	0.9
2.30		1.844	1.521	1.291	1.209	0.9
0.30		1.741	1.497	1.329	1.298	0.9
1.00		4.113	3.536	3.140	3.066	0.9
1.30	C9	4.683	4.026	3.576	3.491	0.9
2.00		5.468	4.701	4.175	4.076	0.9
2.30		5.652	4.859	4.315	4.214	0.9
0.30		3.300	3.130	3.033	2.837	0.9
1.00		7.797	7.394	7.166	6.703	0.9
1.30	C10	8.878	8.419	8.160	7.632	0.9
2.00		10.365	9.830	9.527	8.911	0.9
2.30		10.714	10.160	9.847	9.211	0.9
0.30		3.402	3.144	2.982	2.931	0.9
1.00		8.039	7.428	7.045	6.925	0.9
1.30	C11	9.153	8.457	8.022	7.884	0.9
2.00		10.686	9.874	9.366	9.205	0.9
2.30		11.046	10.207	9.681	9.575	0.9

Table 3: Theoretical computation of functional parameters in individual hydrocarbon diffusion

		$\left(1-\frac{C_{HCW}}{C_{HC}}\right)_A$	$\left(1-\frac{C_{HCW}}{C_{HC}}\right)_B$	$\left(1-\frac{C_{HCW}}{C_{HC}}\right)_C$	$\left(1-\frac{C_{HCW}}{C_{HC}}\right)_D$	$In\left(1-\frac{C_{HCW}}{C_{HC}}\right)_A$	$In\left(1-\frac{C_{HCW}}{C_{HC}}\right)_B$	$In\left(1-\frac{C_{HCW}}{C_{HC}}\right)_C$	$In\left(1-\frac{C_{HCW}}{C_{HC}}\right)_D$
C6	0.30	0.255	0.692	0.273	0.278	-0.294	-1.178	0.319	-0.348
	1.00	0.667	1.538	0.636	0.667	-1.100	-	-1.011	-1.100
	1.30	0.765	1.769	0.773	0.778	-1.448	-	-1.483	-1.505
	2.00	0.882	2.079	0.909	0.889	-2.137	-	-2.397	-2.198
	2.30	0.922	2.154	0.909	0.944	-2.551	-	-2.397	-2.882
C7	0.30	0.285	0.284	0.286	0.282	-0.335	-.0334	-0.337	-0.331
	1.00	0.669	0.668	0.671	0.671	-1.106	-1.103	-1.112	-1.118
	1.30	0.765	0.763	0.764	0.764	-1.448	-1.440	-1.444	-1.444
	2.00	0.892	0.889	0.893	0.900	-2.226	-2.198	-2.235	-2.303
	2.30	0.923	0.921	0.921	0.918	-2.564	-2.538	-2.538	-2.501
C8	0.30	0.284	0.284	0.284	0.284	-0.334	-0.334	-0.334	-0.334
	1.00	0.671	0.671	0.671	0.671	-1.112	-1.112	-1.112	-1.112
	1.30	0.764	0.764	0.764	0.764	-1.444	-1.444	-1.444	-2.227
	2.00	0.892	0.892	0.892	0.892	-2.226	-2.226	-2.226	-2.226
	2.30	0.922	0.922	0.922	0.922	-2.551	-2.551	-2.551	-2.551
C9	0.30	0.284	0.284	0.284	0.283	-0.334	-0.334	-0.334	-0.334
	1.00	0.671	0.671	0.671	0.671	-1.112	-1.112	-1.112	-1.112
	1.30	0.764	0.764	0.764	0.764	-1.444	-1.444	-1.444	-1.444
	2.00	0.892	0.892	0.892	0.892	-2.226	-2.226	-2.226	-2.226
	2.30	0.922	0.922	0.922	0.922	-2.551	-2.551	-2.551	-2.551
C10	0.30	0.284	0.284	0.284	0.284	-0.334	-0.334	-0.334	-0.334
	1.00	0.671	0.671	0.671	0.671	-1.112	-1.112	-1.112	-1.112
	1.30	0.764	0.764	0.764	0.764	-1.444	-1.444	-1.444	-1.444
	2.00	0.892	0.892	0.892	0.892	-2.226	-2.226	-2.226	-2.226
	2.30	0.922	0.922	0.922	0.922	-2.551	-2.551	-2.551	-2.551
	0.30	0.284	0.284	0.284	0.284	-0.334	-0.334	-0.334	-0.334

	1.00	0.671	0.671	0.671	0.671	-1.112	-1.112	-1.112	-1.112
C11	1.30	0.764	0.764	0.764	0.764	-1.444	-1.444	-1.444	-1.444
	2.00	0.892	0.892	0.892	0.892	-2.226	-2.226	-2.226	-2.226
	2.30	0.922	0.922	0.922	0.922	-2.551	-2.551	-2.551	-2.551

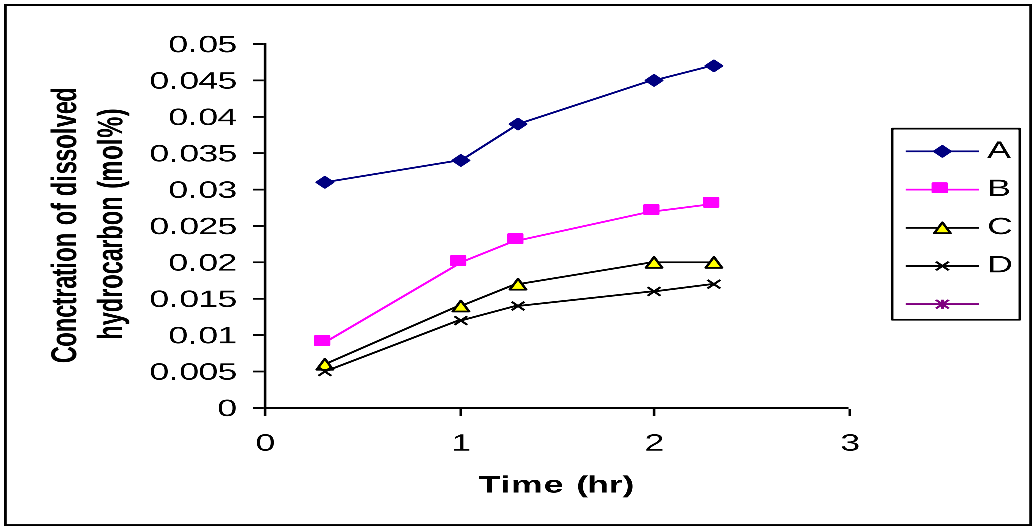

Figure 4 illustrates the temporal variation in the concentration of dissolved hydrocarbon (C6) across different sample sets. Each sample represents a unique environmental condition or treatment level, allowing for a comprehensive understanding of how time influences hydrocarbon dissolution in the samples. The x-axis denotes time, while the y-axis displays the concentration levels of C6, enabling a visual comparison of the hydrocarbon dynamics over the observed period. This data is crucial for understanding the behavior of dissolved hydrocarbons in various contexts, such as ecological impacts and remediation processes.

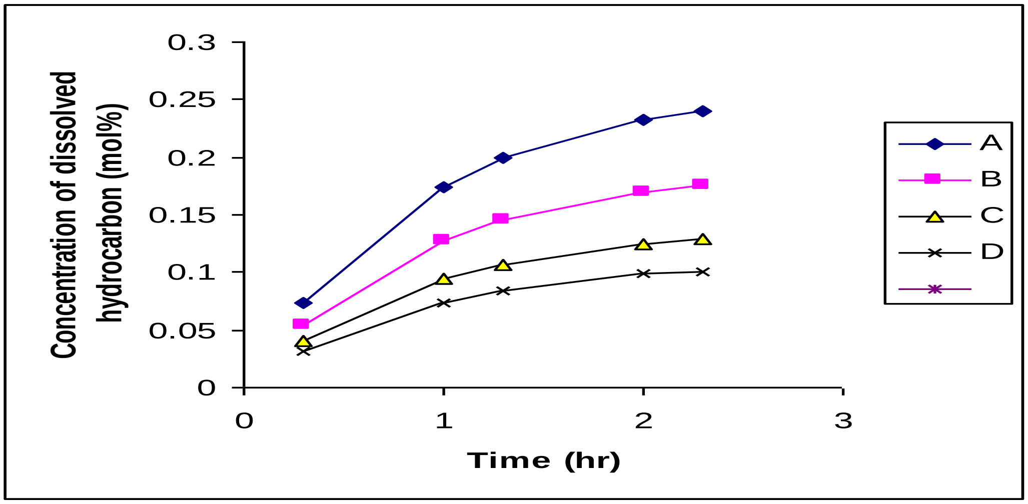

Figure 5 illustrates the concentration of dissolved hydrocarbon, specifically C7, plotted against time for a series of different samples. This graph provides insights into how the levels of C7 hydrocarbons evolve, highlighting any notable trends or variations in concentration across the samples tested. The data reflects the effects of environmental factors, sample composition, and potential degradation processes on the concentration of these hydrocarbons, allowing for a better understanding of their behavior in various conditions.

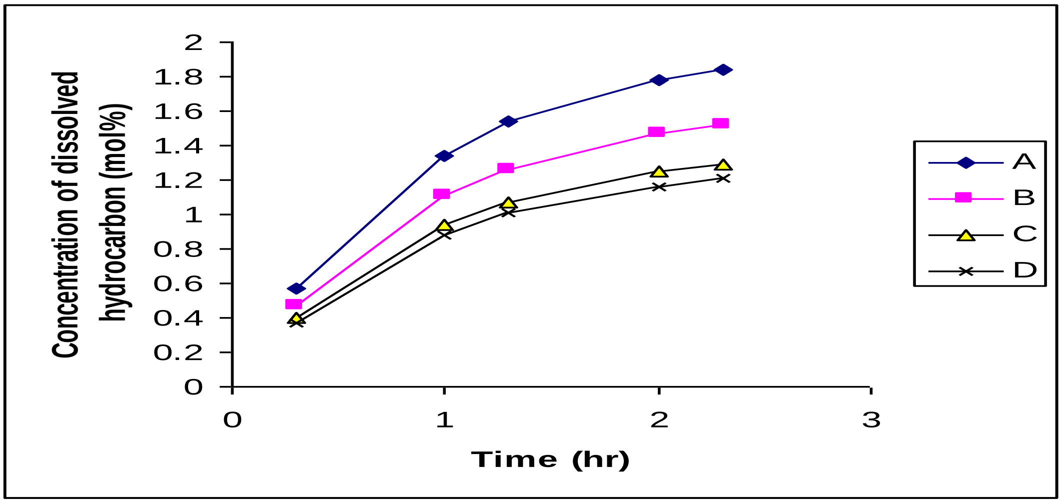

Figure 6 illustrates the concentration of dissolved hydrocarbons, specifically C8, plotted against time for a range of different samples. The graph effectively showcases how the concentration levels of C8 vary over time across these samples, providing insights into the kinetics of hydrocarbon dissolution in the tested environments. This data is crucial for understanding the behavior of hydrocarbons in natural and contaminated waters, as well as for evaluating environmental impacts and recovery strategies.

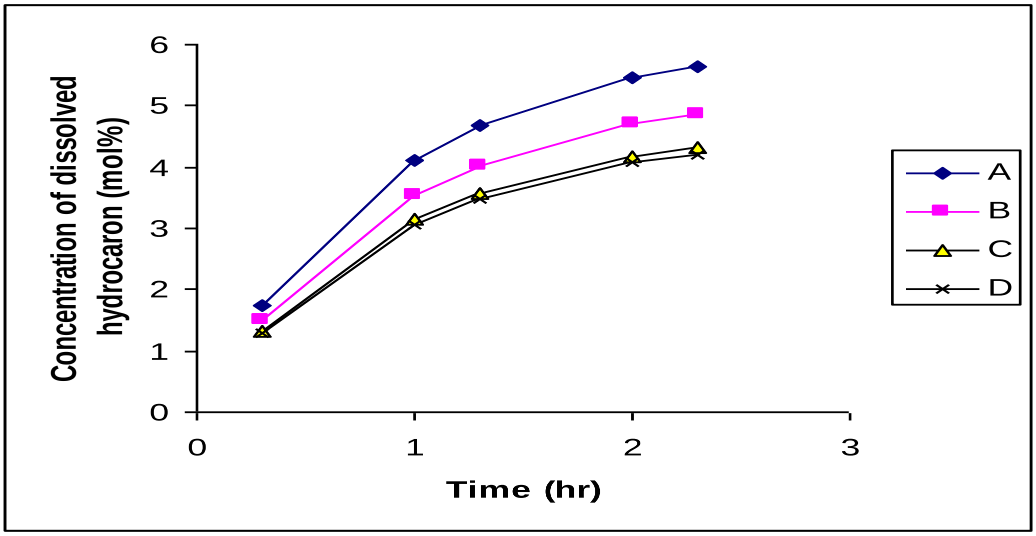

Figure 7 illustrates the temporal concentration of dissolved hydrocarbons, specifically C9, across various sample sets. The graph plots the concentration levels on the y-axis against time on the x-axis, showcasing the dynamic changes in hydrocarbon levels over the observed period. Each sample is denoted distinctly, allowing for comparative analysis of C9 concentrations across different conditions or locations. This detailed depiction helps in understanding the environmental impacts and behavior of dissolved hydrocarbons in the analyzed samples.

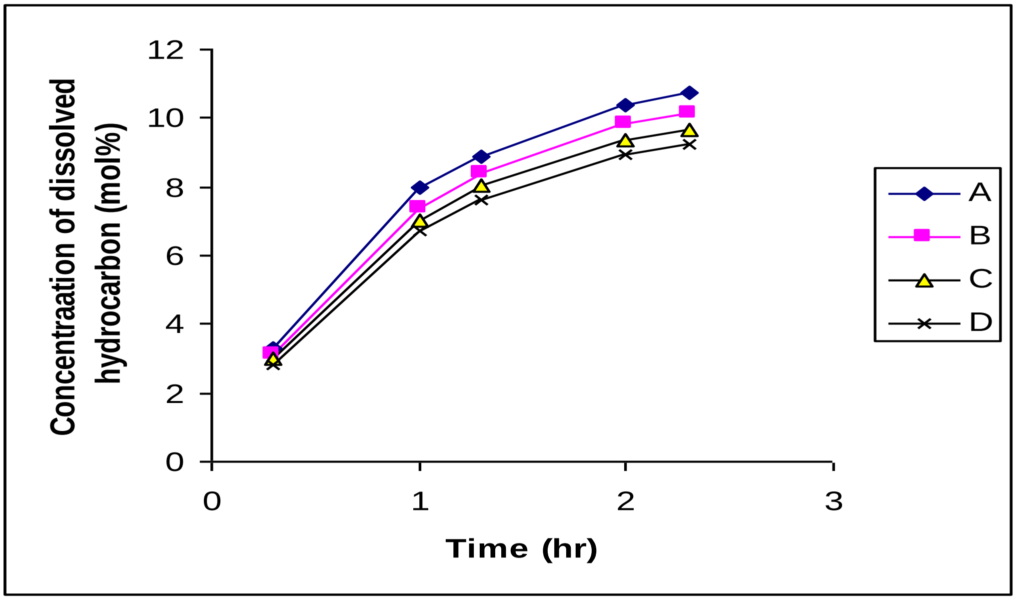

Figure 8 illustrates the temporal concentration of dissolved hydrocarbons, specifically C10, across various sample sets. The graph plots the concentration levels on the y-axis against time on the x-axis, showcasing the dynamic changes in hydrocarbon levels over the observed period. Each sample is denoted distinctly, allowing for comparative analysis of C10 concentrations across different conditions or locations. This comprehensive depiction helps in understanding the environmental impacts and behavior of dissolved hydrocarbons in the analyzed samples.

The results obtained from the investigation are presented in Tables and Figures. From Table 1 the relationship of individual hydrocarbon concentration was illustrated. Considering the results illustrated in Table 2 for the concentration of dissolved individual hydrocarbon $C_{HCW} = C_{HC} - C_{HC} \exp -t/\tau$ at the constant coefficient of $\tau = 0.9$, for various time intervals indicate an increase in the dissolution rate of individual hydrocarbon. Similarly, Table 3 illustrates the mathematical computation of the $1 - \frac{C_{HCW}}{C_{HC}}$ for and the In $(1 - \frac{C_{HCW}}{C_{HC}})$ for each component was commutated as shown for each of the sample components of A, B, C, and D, and results obtained indicate an increase in $1 - \frac{C_{HCW}}{C_{HC}}$ with an increase in time for the various sampling components. The results presented in Figures 4 to 8 illustrate an increase in the concentration of dissolved hydrocarbon of individual hydrocarbon in the system upon the influence of time. It is seen that the rate of diffusion of the individual hydrocarbon is influenced by time and the nature of the contaminants as presented in the tables and Figures of this research work. The behavior of Figures 4 to 8 is the same but the concentration in terms of mole percent is different, the variances in the mole percent of the individual hydrocarbon can be attributed to the variation in the molecular weight as well as environmental factors.

3. Conclusion

The following conclusion was drawn from the investigation: Concentration has a key impact on the rate of diffusion of individual hydrocarbons and is also influenced by the concentration. Higher concentrations of specific condensate fractions lead to increased molecular interactions, automatically altering diffusion dynamics. The coefficient of time is another important factor that influences it. the rate of diffusion. The diffusion process is time-dependent, with the coefficient of time playing a critical role in determining the extent of mass transfer. Over prolonged durations, molecular distribution within the medium stabilizes, affecting the overall dispersion rate. The characteristics of the individual hydrocarbon influence the rate of diffusion. The physicochemical properties of individual natural gas condensate compounds, such as molecular weight, volatility, and polarity, significantly influence their diffusion rates. Lighter fractions exhibit faster diffusion compared to heavier, more complex hydrocarbon structures. The ratio of water in oil composition influences the rate of diffusion of the hydrocarbon. This study provides significant insights into the diffusion behavior of natural gas condensates in various marine environmental and processing conditions. Based on the experimental and analytical findings, the above conclusions are drawn, these findings provide valuable knowledge for understanding the behavior of natural gas condensates in marine environment systems, aiding in environmental risk assessment, spill mitigation strategies, and optimization of treatment processes in petroleum industries.

References

Adaku, J. E., Henry, F. O. and Olayinka, I. (2022): Air Pollution, Climate Change, and Ecosystem Health in the Niger Delta: *International Journal of Environmental Science and Technology (IJEST)*. 11(11), 525. https://doi.org/10.3390/socsci11110525.

Adewusi, V. A., & Ilori, T. A. (2012). *Gas flaring in Niger Delta region of Nigeria: Cost, ecological and human health implications. Environmental Management and Sustainable Development*, 1(1), 187–204. macrothink.org

Afolabi, S. A., Ayodele, O. A. and Samuel, O. A, (2020): Modeling natural gas viscosity for Niger Delta Region using artificial neural network. *International Journal of Research and Engineering Studies (IJRES).* 10(3), 50-61.

Aprioku, P. C., Akpa, J. G., Ademiluyi, T. O., & Ehirim, E. N. (2023). Petroleum exploration, exploitation, spill and diffusion of crude oil in the marine environment: A review. *American Journal of Engineering Research*, 13(6), 98–110.

Aust, S. D., Swaner, P. R., & Stahl, J. D. (2004). Detoxification and metabolism of chemicals by white-rot fungi. *Pesticide Decontamination and Detoxification*, 863, 3–14.

Blunt, J. W., Copp, B. R., Munro, M. H. G., Northcote, P. T., & Prinsep, M. R. (2004). Marine natural products. *Natural Products Reports*, 21, 1–49.

Botwe, T., & Akpabio, I. O. (2020). Correlation of natural gases from the X field of the Niger Delta, Nigeria. *Journal of Energy Research and Reviews*, 4(3), 1–12.

Ifeoluwa O. A., Oluwaseun A. A. and Oluwatobi A. O. (2019). Optimizing gas production strategy in offshore Niger Delta Gas Condensate Field using dynamic simulation model. *Journal of Environmental Science and Technology*.

Oburoh, A. O., Oforka, A. E. and Chukwu, C. O. (2017): Laboratory assessment on the rate of diffusion of spilled Oil in marine sediment. *International Journal of Innovative Science, Engineering & Technology* (IJISET). 6(7), 1-5.

Ojo, A. O., & Tse, C. A. (2023). Geo-mechanical and geo-morphology characterization of the cap rock *in* the Niger Delta for potential carbon sequestration. *Scientific Reports*, 13, Article 12345.

Orodu, O. D., & Orodu, K. B. (2011). *Predictive models for condensate gas ratio (CGR) – Part 1.* *Current Journal of Applied Science and Technology*, 1(3), 118–140. journalcjast.com